



## Characterization of Strange Attractors of Lorenz Model of General Circulation of the Atmosphere

C. MASOLLER,\* A.C. SICARDI SCHIFINO\* and L. ROMANELLI\*\*

\*Instituto de Física, Facultad de Ciencias, Tristán Narvaja 1674 Montevideo, Uruguay  
 and Instituto de Física, Facultad de Ingeniería Herrera y Reissig 565 Montevideo, Uruguay.

\*\*Departamento de Física, F.C.E. y N., U.B.A, Ciudad Universitaria (1428) Buenos Aires, Argentina.

**Abstract** - The dynamics of the Lorenz model of general circulation of the atmosphere is investigated. The attractors found are characterized by calculating their Fourier spectra, Lyapunov exponents and dimensions. In addition, the self similarity of the attractors is studied with the aid of a Poincaré map. A series of one-dimensional maps derived from the Poincaré section illustrates the structural changes of the attractors as a function of parameters variations.

### 1. INTRODUCTION

The search for chaotic dynamics has become a fascinating subject in many scientific disciplines, and a great deal of interest has been focused on the relevance of strange attractors in modeling real systems. Numerical and theoretical evidence for strange attractors has been found in many model equations, and several techniques to analyze chaotic dynamics have been developed [1,2]. In order to compare model calculations with experimental data, the characterization of the geometrical and statistical properties of the strange attractors is required. In the present paper we present such study of chaotic attractors of the Lorenz model, a model of considerable importance in the fields of meteorology, fluid dynamics and atmospheric sciences.

In Refs. [3,4] Lorenz introduced a modified version of his famous Lorenz equations [5], a low-order geostrophic baroclinic model capable of representing the general circulation of the atmosphere. In previous studies we have shown that this model exhibits very rich dynamics [6,7]. An immense variety of bifurcation sequences were found, and coexistence of several attractors was reported. In the present contribution we characterize qualitatively these strange attractors, and investigate period-doubling cascades leading to chaos.

Lorenz model of general circulation of the atmosphere consists of the following nonlinear ordinary differential equations [3,4]

$$\frac{dX}{dt} = -Y^2 - Z^2 - aX + aF \quad (1)$$

$$\frac{dY}{dt} = XY - bXZ - Y + G \quad (2)$$

$$\frac{dZ}{dt} = bXY + XZ - Z \quad (3)$$

where the variable  $X$  represents the strength of a large-scale westerly-wind current, while  $Y$  and  $Z$  are the strengths of the cosine and sine phases of a chain of superposed waves. The parameter  $F$  represents the external-heating contrast, and  $G$  represents the heating contrast between oceans and continents. For  $a = 1/4, b = 4, G = 1$  and different intensities of the external thermal forcing  $F$ , these equations may have one or more stable solutions, which can be steady-states, periodic solutions, or aperiodic solutions.

We will now describe briefly the changes that occur in the qualitative nature of the attractors as the parameter  $F$  is varied [6,7]. For  $F < 1.18$  the equations possess one stable steady-state solution (fixed point 1), for  $1.18 < F < 1.27$  two stable steady state solutions (fixed points 1 and 2), and for  $1.27 < F < 4.31$  one stable steady state (fixed point 1) and one periodic solution (weak limit cycle). The weak cycle period-doubles at  $F = 6.25$  and becomes unstable at  $F = 7.85$ . In the region  $4.31 < F < 7.85$  the model presents two different attractors (the weak cycle and the strong attractor) and the diagram of solutions becomes extremely complicated. There are regions of the parameter  $F$  in which the strong attractor is periodic, regions in which it is aperiodic, and regions in which it does not exist, or is barely stable and only the weak limit cycle exists. In the turbulent region  $7.85 < F < 8.0$  the weak cycle is unstable and the equations have only aperiodic solutions.

We will study in detail three of the strong chaotic attractors found in [7] attractor  $B$  ( $F = 4.56$ ), attractor  $N$  ( $F = 5.198$ ) and the strongly chaotic attractor ( $F = 8.0$ ). While the transition scenarios of attractors  $B$  and  $N$  are period-doubling cascades, the strongly chaotic attractor is born when a long chaotic transient becomes stable after the subcritical Hopf bifurcation of the weak limit cycle. The qualitative nature of these attractors is studied with the aid of phase portrait and power spectrum analysis [1,2,8]. We find that attractors  $B$  and  $N$  look like "noise limit cycles". In contrast, the dynamics in the last one is highly chaotic. In addition, the Poincaré section of the strongly chaotic attractor presents the self-similar structure characteristic of strange attractors [9] and is considerably more complicated than the Poincaré sections of attractors  $B$  and  $N$ . The spectrum of Lyapunov exponents [10-12] and several dimensions [13-16] are employed for dynamical and geometrical characterization. We show that these attractors have one positive Lyapunov exponent and fractal dimension. In addition, the period doubling cascades found in [7] are studied in detail. We show that these routes are in perfect correspondence to the Feigenbaum sequence [17,18]. A series of one dimensional maps is derived from the Poincaré section that explains this behavior.

The paper is organized as follows. In section 2 the phase portrait and power spectrum of the attractors are studied, and their Poincaré sections are presented in section 3. In section 4 the period-doubling routes to chaos are analyzed. Section 5 is concerned with the dynamical and geometrical characterization with the spectrum of Lyapunov exponents and dimensions. Finally, section 6 presents the discussion of the results.

## 2. VISUALIZATION OF THE DYNAMICS

In order to study the qualitative nature of attractors  $B$ ,  $N$  and the strongly chaotic attractor, we use two of the more commonly employed methods, namely phase portraits and power spectrum. The phase plots were obtained integrating equations (1)-(3) and plotting  $X(t)$  vs.  $Z(t)$ , after letting transients relax (the parameters used are  $a = 1/4, b = 4, G = 1$ ). The power spectrum was calculated using 4096 points corresponding to the time series of the variable  $X(t)$  with a time difference  $\Delta t = 0.5$ .

Let us begin by comparing the phase portraits. While the orbits of the attractors  $B$  (Fig.1a) and  $N$  (Fig.1c) look like "noisy limit cycles", the orbit of the strongly chaotic attractor (Fig.1e) appears to fill out a continuous region of the phase space and has a considerably more complicated structure. This impression is reaffirmed by the examination of the power spectrum. The spectrum of attractors  $B$  (Fig.1b) and  $N$  (Fig.1d) is composed of broadband components and sharp peaks. In contrast, in the spectrum of the strongly chaotic attractor (Fig.1f) we do not distinguish any sharp peaks. These results agree with the fact that attractors  $B$  and  $N$  arise from period multiplication cascades

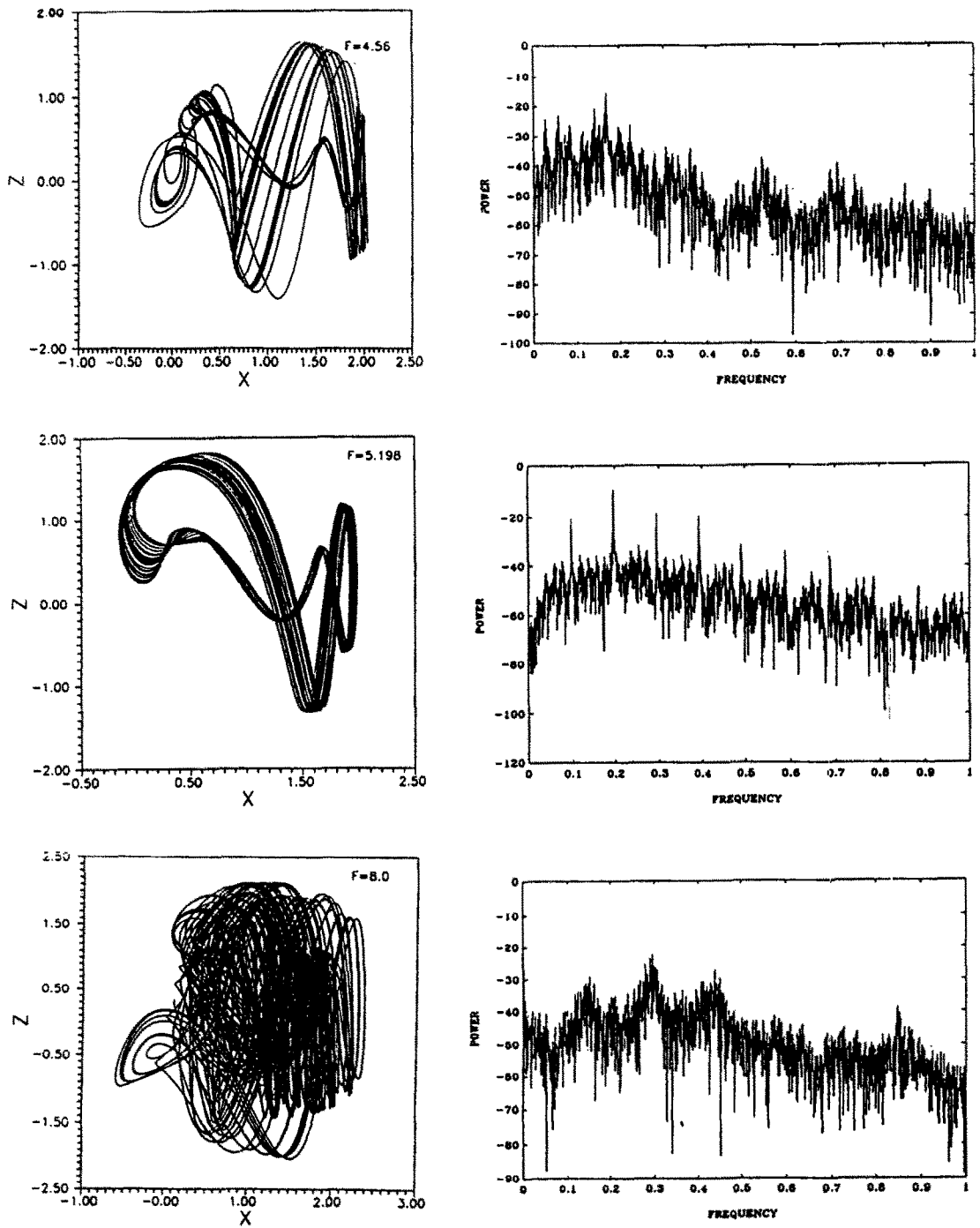


Fig. 1 Phase plots and power spectra of attractors B, N and turbulent attractor. Parameters:  $a=1/4$ ,  $b=4$ ,  $G=1$   
 (a) and (b)  $F=4.56$ ; (c) and (d)  $F=5.198$ ; (e) and (f)  $F=8.0$ .

of strong limit cycles, while the strongly chaotic attractor is a long chaotic transient that becomes stable when the weak limit cycle loses stability. The transition scenario of attractor  $N$  is a period doubling cascade that will be studied in section 4, and closer examination of Fig. 1d reveals that the spectrum of attractor  $N$  presents sharp peaks at frequencies  $nf_0$  with  $f_0 \approx 0.18$  in the frequency of cycle  $N$ .

### 3. POINCARÉ SECTION ANALYSIS

In order to gain insight into the geometrical structure of the attractors, we use the Poincaré section technique [8]. The Poincaré section is a two-dimensional intersection of the phase space chosen in such a way that all qualitatively interesting trajectories actually intersect the plane transversely. In our case we chose the plane  $Z = 0$  and plot the coordinates  $X$  vs.  $Y$  whenever  $Z = 0$  and  $dZ/dt > 0$  ("mirror" points are rejected). For the precise location of the intersection point an effective technique proposed by Hénon was employed [19].

Figure 2a shows the Poincaré section of attractor  $B$ . Five strips can be seen in the figure. Figs. 2b, 2c and 2d are blowups of sectors of the section at successively greater resolution. This attractor shows the recursive structure that occurs on fractal attractors [9]. A careful observation of Fig. 3d suggests that there are sectors of the map slightly more probable than others, and that this attractor is a fractal [14].

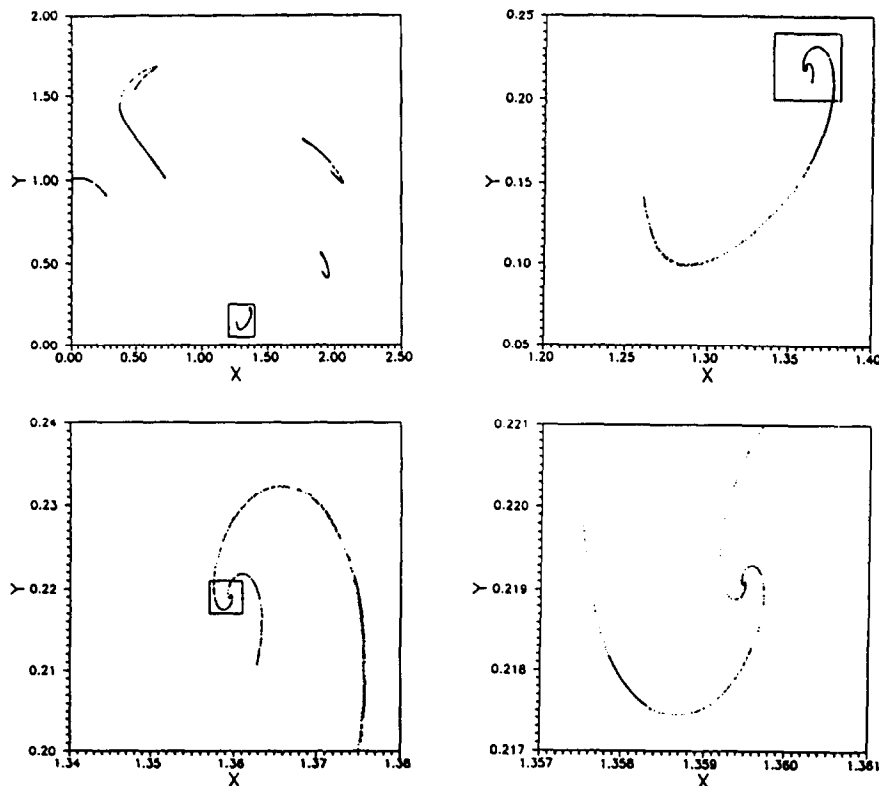


Fig. 2 (a) Poincaré section of attractor B ( $F=4.56$ ). Figures (b)-(d) are blowups constructed by plotting only those points that lie within the box indicated in figs. (a)-(c). Fig. 2a contains 5000 points, while (b)-(d) were constructed from 400,000.

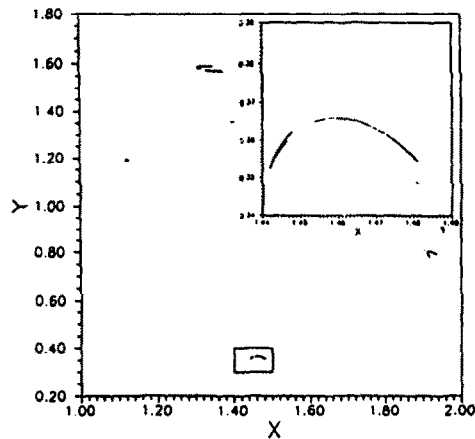


Fig. 3 (a) Poincaré section of attractor  $N$  ( $F=5.198$ ). (b) Blowup of the box indicated in fig. 3a.

Figure 3a shows the Poincaré section of attractor  $N$ , and Fig. 3b is a magnification of the sector indicated in Fig.3a. We see that this attractor consists of three distinct arcs and has simpler structure than the attractor  $B$ . A series of one-dimensional maps derived in the next section, from this Poincaré map will add us in explaining the sequence of bifurcations observed.

Figure 4a shows the Poincaré section of the strongly chaotic attractor, and Figs. 4b, 4c and 4d are successively magnification at greater resolution of a sector of the map. This attractor has pronounced sheet-like Cantor set structure characteristic of chaotic attractors.

#### 4. PERIOD-DOUBLING ROUTES TO CHAOS

The routes into chaotic dynamics are studied by means of the Poincaré maps defined in the previous section. In [6,7] a sequence of saddle-node and inverse saddle node bifurcations, giving rise to a periodic window structure, was found.

Each periodic window is the domain of a different strong limit cycle and the transition scenario is usually a subharmonic cascade. In this section we will describe three of the period-doubling cascades found in the first part of this series and show that the essential dynamics can be captured by a one-dimensional non-invertible map.

In the first window of periodicity, cycle  $B$  period-doubles at  $F = 4.484$  and follows the subharmonic cascade shown in the bifurcation diagram of figure 5a. This bifurcation diagram was obtained plotting the coordinate  $X$  of points in a sector of the Poincaré map, as a function of  $F$ . We observe that the range of the Poincaré section that is visited by the chaotic trajectory grows with increasing the parameter  $F$ . Before the end of the Feigenbaum sequence we observe a sharp interior crisis at  $F = 4.488$  and the size of the chaotic attractor suddenly grows. Beyond this value of  $F$  we observe a broad continuation of the chaotic regime up to another crisis at  $F = 4.489$  that leads to a sudden destruction of the attractor.

In the second window of periodicity, cycle  $K$  period-doubles at  $F = 4.601$  and follows a period-doubling cascade that is interrupted by a period-halving cascade.

The corresponding bifurcation diagram is shown in Fig. 5b. In the third window cycle  $N$  period doubles at  $F = 5.0602$  and follows the period doubling cascade illustrated in Fig. 5c. Before the end of the Feigenbaum sequence, a crisis occurs at  $F = 5.089$  and leads to a sudden destruction of the chaotic attractor.

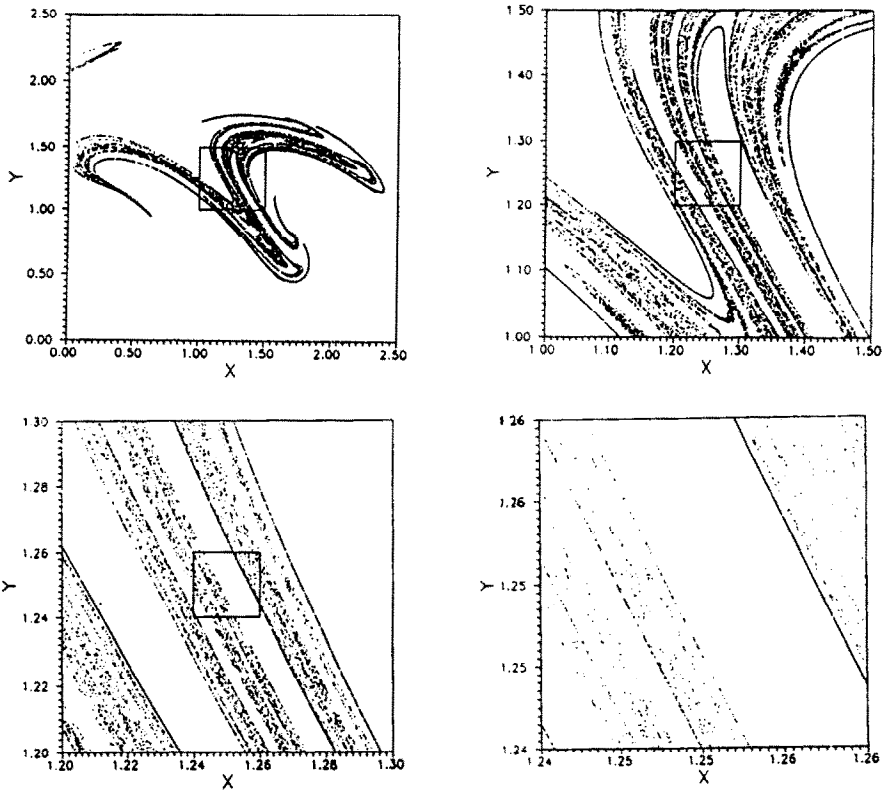


Fig. 4 Poincaré section of the turbulent attractor. The blowups shown in figs (b)-(d) are constructed by plotting only those points that lie within the box indicated in figs. (a)-(c). Figure 4a contains only 10000 points, while (b), (c) and (d) were constructed from 1,000,000 points.

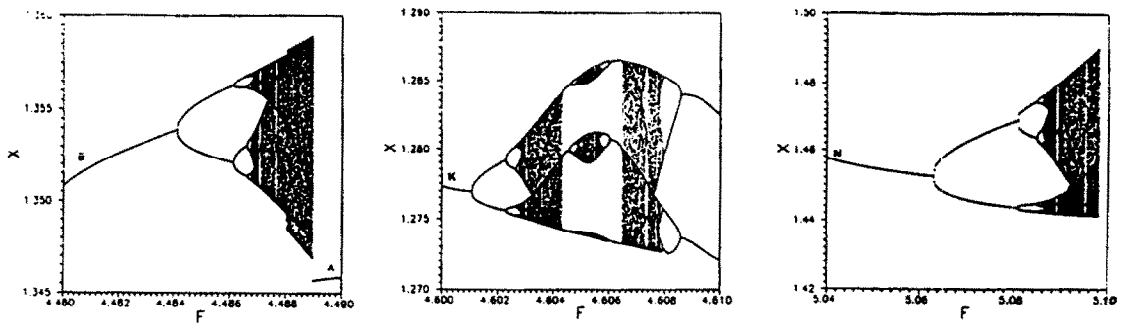


Fig. 5 (a) Bifurcation diagram of cycle B; (b) Bifurcation diagram of cycle K.; (c) Bifurcation diagram of cycle N.

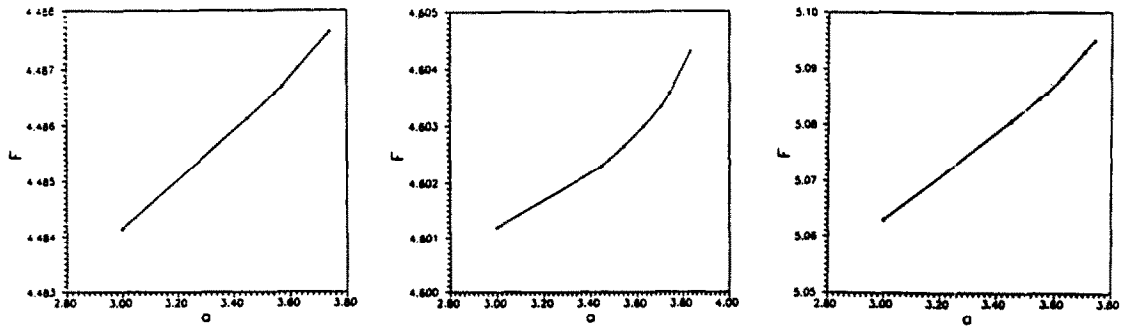


Fig. 6 Relation between the critical values of the parameter  $a$  in the Feigenbaum's sequence of bifurcations and the values of the parameter  $F$  at which the analogous events occur in the dynamics of the model. a) Bifurcations of cycle B. b) Bifurcations of cycle K. c) Bifurcations of cycle N.

The first part of the three bifurcation diagrams resembles the structure of the attractors of the logistic map on the unit interval  $X_{n+1} = aX_n(1 - X_n)$  [17,18]. Moreover, there is an almost linear relation between the values of the parameter  $a$  and the parameter  $F$  at which the period doublings and periodic windows in the chaotic regime occur (see Fig.6). The sequence of events leading into chaos and the fine structure of the chaotic regime along these routes show perfect correspondence to the Feigenbaum or Sharbovski sequence.

For few selected values of  $F$  in the bifurcation cascade of cycle  $N$  we constructed the first return maps on the unit interval, shown in Fig.7. These maps were constructed from points in the sector

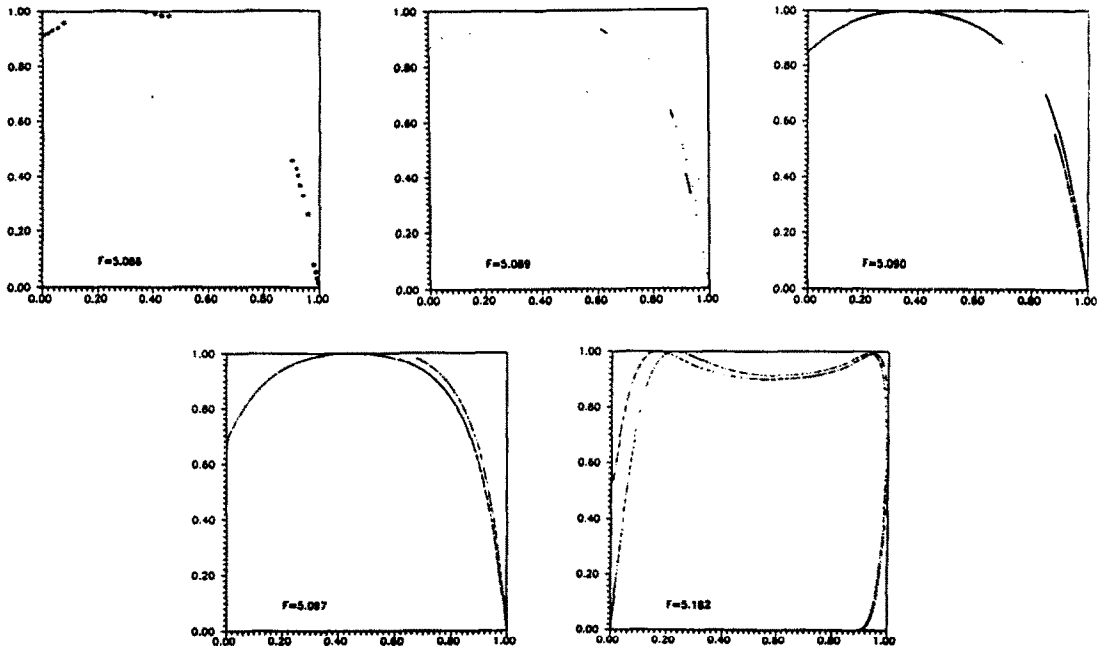


Fig. 7 Return maps  $(w_n, w_{n+1})$  on the unit interval corresponding to the period-doubling cascade of cycle B. The parameters are (a)  $F=5.086$ , (b)  $F=5.089$ , (c)  $F=5.09$ , (d)  $F=5.097$ , (e)  $F=5.182$  The points  $w=0$  and  $w=1$  correspond to the outermost and innermost points of the sector of the Poincaré section indicated in fig. 4.

of the Poincaré map indicated in Fig.3b. The coordinate  $X$  of the outermost point of the sector was defined as  $\omega = 0$  and the coordinate  $X$  of the innermost point was chosen to represent the value  $\omega = 1$ . As expected, the maps resemble the logistic map in the parameter range where we observe the Feigenbaum sequence. However, at higher values of  $F$  the map becomes more complicated.

### 5. CHARACTERIZATION OF THE ATTRACTORS

Lyapunov exponents describe the mean rate of exponential divergence or convergence of initially neighboring trajectories and provide the best quantitative measure of chaotic behavior. A system with one or more positive Lyapunov exponents is defined to be chaotic. We have calculated the Lyapunov exponents using the method proposed by Wolf *et. al.*[10] since this technique yields in a straightforward manner for computing the complete Lyapunov spectrum. The results obtained were double-checked by applying alternative methods such as those given by Benettin *et. al.* [11] and Eckmann *et. al.*[12].

Table I summarize the results obtained. The Lyapunov calculations clearly indicate chaotic behavior, since all the attractors have one positive Lyapunov exponent. Nevertheless, the strongly chaotic attractor presents a considerable larger chaotic dynamics than attractors  $B$  and  $N$ , since its positive exponent is larger than the positive exponent of attractors  $B$  and  $N$  and its negative exponent is smaller than the negative exponent of attractors  $B$  and  $N$ .

In order to study the fractal nature of the attractors quantitatively, we now turn to the calculation of the dimension of the attractors. The method proposed by Grassberger and Procaccia [14,15] leads the determination of the correlation dimension  $D_c$  which is a lower bound on the Hausdorff dimension. The correlation sum:

$$C(r) = \frac{1}{N^2} \{ \text{Number of pairs } (x_i, x_j) \text{ with } |x_i - x_j| < r \} \tag{4}$$

was calculated and the scaling region in  $r$  for which  $C(r) \approx r^\mu$  was located. If  $\mu$  approaches a limiting value  $D_c$  as the embedding dimension is increased,  $D_c$  is identified as the correlation dimension. The correlation dimension was calculated from the three dimensional time series  $x_i(t), y_i(t), z_i(t)$  as well as from the reconstructed series  $x(t_i), x(t_i + \tau), x(t_i + 2\tau)$ , applying the delay method to reconstruct the dynamics from the measurements of a single variable. In both cases 70.000 data points were used, and for the reconstruction of the attractor, a delay time  $\tau = 1$  was chosen. The estimated correlation dimensions appear in Table I. We observe a very good agreement between both calculations. While attractors  $B$  and  $N$  present a correlation dimension  $1 < D_c < 2$ , according with the topological shape of the attractors ("noisy limit cycles"), the strongly chaotic attractor has a correlation dimension  $D_c > 2$  evidencing a more complex dynamics. In addition, the Lyapunov dimension  $D_L$  was calculated from the Kaplan and Yorke's formula

$$D_L = j + \frac{\sum_{i=1}^j \lambda_i}{|\lambda_{j+1}|} \tag{5}$$

where  $j$  is the largest integer for which  $\lambda_1 + \dots + \lambda_j \geq 0$ . For typical attractors it has been conjectured [16] that the Lyapunov dimension is equal to the information dimension and thus gives a value  $D_L \geq D_c$ . Our results are given in Table I.

TABLE I Lyapunov exponents and dimensions for attractors B, N, and strongly chaotic

| Attractor                | Lyapunov Exponents |   |       | $D_L$ | $D_c(1)$ | $D_c(2)$ |
|--------------------------|--------------------|---|-------|-------|----------|----------|
| B (F=4.56)               | 0.07               | 0 | -1.0  | 2.07  | 1.50     | 1.48     |
| N (F=5.198)              | 0.07               | 0 | -0.85 | 2.08  | 1.79     | 1.78     |
| Strongly chaotic (F=8.0) | 0.23               | 0 | -0.59 | 2.39  | 2.23     | 2.22     |

(1) Calculated from the reconstructed time series  $x(t_i), x(t_i + \tau), x(t_i + 2\tau)$  with  $\tau = 1$ .

(2) Calculated from the three dimensional time series  $x_i(t), y_i(t), z_i(t)$

## 6. DISCUSSION

In this contribution we have presented a full characterization of the chaotic attractors of the Lorenz model of general circulation of the atmosphere.

Direct evidence from the inspection of computed trajectories shows that attractors  $B$  and  $N$  look like "noisy limit cycles", while the strongly chaotic attractor presents a much more complicated structure. In addition the spectra of attractors  $B$  and  $N$  present sharp peaks and broad-band components. On the contrary, in the spectrum of the strongly chaotic attractor we discern no sharp peaks. These features confirm the results of ref. [7] while the transition scenarios of attractors  $B$  and  $N$  are period-multiplication cascades, the transition scenario of the strongly chaotic attractor is a subcritical Hopf bifurcation of the weak limit cycle.

Moreover, the Poincaré sections of attractors  $B$  and  $N$  consist of thin arcs while the Poincaré section of the strongly chaotic attractor presents a complicated self-similar sheet-like structure. With the aid of Poincaré sections the period doubling cascades were studied in detail. We were able to show that chaos develops in an almost perfect Feigenbaum scenario. However, the chaos is never fully developed, but it ends with a crisis or a period-halving cascade. The detailed study of these crises is the object of a forthcoming paper.

Dimension and Lyapunov exponent calculations confirm the fractal and chaotic nature of the attractors. The Lyapunov exponents and dimensions of attractors  $B$  and  $N$  are quantitatively different from those of the strongly chaotic attractor. The values are lower, indicating much thinner strange attractors.

*Acknowledgment* This work was supported in part by the "Proyecto Tecnológico CONICYT-BID" of the Consejo Nacional de Investigaciones Científicas y Técnicas (CONICYT, URUGUAY); by PEDECIBA (Project URU/84/002 - UNDP) and Comisión Sectorial de Investigación Científica (CSIC, URUGUAY) and by PID 3-00571/88 (CONICET, ARGENTINA)

## REFERENCES

1. H.G. Schuster, *Deterministic Chaos, An Introduction* 2nd. Ed. (VCH, Weinheim, 1988).
2. Hao Bai-Lin, *Elementary Symbolic Dynamics and Chaos in Dissipative Systems* (World Scientific, Singapore, 1989).
3. E. N. Lorenz, *Tellus* 36A (1984) 98.
4. E. N. Lorenz, *Tellus* 42A (1990) 378.
5. E. N. Lorenz, *J. Atmos. Sci.* 20 (1963) 130.
6. C. Masoller, A. Sicardi and L. Romanelli, *Physics Letters A* 167 (1992) 185.
7. C. Masoller, A. Sicardi Schifino and L. Romanelli, submitted to *Journal of the Atmospheric Sciences*
8. P. Bergé, Y. Pomeau and C. Vidal, *Order Within Chaos* (Wiley, 1986).
9. B.B. Mandelbrot, *The Fractal Geometry of Nature* (W.H. Freeman, New York, 1983)
10. A. Wolf, J.B. Swift, H.L. Swinney and A. Vastano, *Physica D* 16 (1985) 285.
11. G. Benettin, L. Galgani, A. Giorgilli and J. M. Strelcyn, *Meccanica* 15 (1980) 9.

12. J-P. Eckmann, S.O. Kamphorst, D. Ruelle and S. Ciliberto, *Phys. Rev. A* **34** (1986) 4971.
13. J.D. Farmer, E. Ott, J.A. Yorke, *Physica D* **7** (1983) 153
14. P. Grassberger, I. Procaccia, *Physica D* **9** (1983) 189.
15. P. Grassberger and I. Procaccia, *Phys. Rev. Lett.* **50** (1983) 346.
16. J.L. Kaplan and J.A. Yorke, *Lecture Notes in Mathematics* **730** (Springer-Verlag, 1979) p. 228; P. Frederickson, J. Kaplan, E. Yorke and J. Yorke, *J. Diff. Eqs.* **49** (1983) 185.
17. M.J. Feigenbaum, *J. Stat. Phys.* **19** (1978) 25; *J. Stat. Phys.* **21** (1979) 669.
18. P. Collet and J-P Eckmann, *Iterated Maps in the Interval as Dynamical Systems* (Birkhauser, Boston, 1980).
19. M. Hénon, *Physica D* **5** (1983) 412.